Jason Potratz

Jingzhou Yang[1]
Phone: 1-319-353-2249
e-mail: jyang@engineering.uiowa.edu

Virtual Soldier Research (VSR) Program,
Center for Computer-Aided Design,
The University of Iowa,
111 Engineering Research Facility,
Iowa City, IA 52242-1000

Karim Abdel-Malek
Virtual Soldier Research (VSR) Program,
Center for Computer-Aided Design,
and Department of Biomedical Engineering
The University of Iowa,
Iowa City, IA 52242-1000

Esteban Peña Pitarch
Department Enginyeria Mecanica,
Universitat Politecnica de Catalunya (UPC),
Av. Bases de Manresa, 61-73,
08240 Manresa, Spain

Nicole Grosland
Virtual Soldier Research (VSR) Program,
Center for Computer-Aided Design,
and Department of Biomedical Engineering,
and Department of Orthopaedic Surgery
and Rehabilitation,
The University of Iowa,
Iowa City, IA 52242-1000

A Light Weight Compliant Hand Mechanism With High Degrees of Freedom

This paper presents the design and prototyping of an inherently compliant lightweight hand mechanism. The hand mechanism itself has 15 degrees of freedom and five fingers. Although the degrees of freedom in each finger are coupled, reducing the number of independent degrees of freedom to 5, the 15 degrees of freedom of the hand could potentially be individually actuated. Each joint consists of a novel flexing mechanism that is based on the loading of a compression spring in the axial and transverse direction via a cable and conduit system. Currently, a bench top version of the prototype is being developed; the three joints of each finger are coupled together to simplify the control system. The current control scheme under investigation simulates a control scheme where myoelectric signals in the wrist flexor and extensor muscles are converted in to x and y coordinates on a control scheme chart. Static load-deformation analysis of finger segments is studied based on a 3-dimensional model without taking the stiffener into account, and the experiment validates the simulation. [DOI: 10.1115/1.2052805]

Keywords: High Degree of Freedom, Hand Mechanism, Compliant Lightweight Mechanism

Introduction

An artificial human-like hand based on a new design would fulfill different needs. There are numerous robotics applications that would benefit from an anthropometrically shaped device, a "gripper," capable of grasping and manipulating objects. Other grippers, often as simple as a one degree of freedom (DOF) pinching device, are used successfully in many applications, but a gripper that accurately reproduces human motion and grasping postures is novel and would be beneficial. For instance, in cases where the environment prevented or inhibited a human from completing a task, a robotic hand could be used as part of a system to complete the task. If humanoid robots were ever to become a reality, then a human-like hand would become a necessity. These robots would interact in the same environment as humans and therefore manipulate the same objects that would be designed with the intention of being manipulated by human hands.

Another central need that would be fulfilled by a new artificial human-like hand would be advanced prosthetics. The ideal replacement for a missing human hand that accurately mimics a human hand in appearance, dexterity, tactile feedback to the user, and simplicity of use, remains far from a reality. Currently available myoelectric robotic prosthetic hands, which typically only have a few DOFs fall far short of this ideal prosthetic hand in terms of appearance, functionality, and ease of use. Surveys [1,2] conducted on user satisfaction of myoelectric hands show that 30–50% of users do not use their hands regularly. The reasons for this lack of use are: low functionality, unsatisfactory cosmetics partly caused by unnatural motion, and low controllability. From a mechanics perspective, even these relatively simple hands are not natural to control; users have to exert an enormous amount of concentration for even simple tasks [3].

In this work we developed a five-fingered hand with 15 DOFs that mimics a human hand in terms of appearance, motion, and grasping ability. One key feature that makes this hand more advanced than any other multifingered hands is the mechanism used for the joints that are similar to the elastic manipulator [4]. This newly developed mechanism is based on the loading of a compression spring in both the axial and transverse directions and offers several advantages over a hand mechanism based on rigid links and revolute joints. Since the structure of each finger is primarily made up of compression springs, the majority of the volume of each finger is occupied by empty space. Thus, the potential for constructing a very light hand exists if the proper materials are used along with an efficient design. A lightweight design is a critical aspect of a comfortable, wearable prosthetic devise and offers obvious advantages for robotics applications, such as smaller actuators and less power consumption. The unique mechanism also allows the hand to be inherently compliant. This characteristic enables the fingers to naturally conform to the shape

[1]To whom correspondence should be addressed.

Contributed by the Bioengineering Division for publication in the JOURNAL OF BIOMECHANICAL ENGINEERING. Manuscript received by the Bioengineering Division March 31, 2005; revision received August 12, 2005. Associate Editor: Mary Frecker.

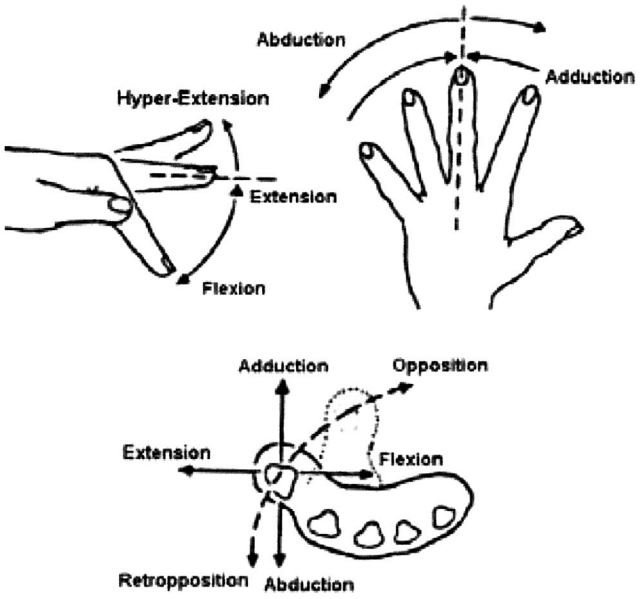

Fig. 1 Degrees of freedom of fingers (see Ref. [15])

of the object that the hand is grasping. This makes for a more secure grip without deliberately adjusting the defection of each joint to achieve the desired shape. The joint mechanisms are actuated by a series of cables and conduits that allow the motors that actuate the joints to be located off the hand, also increasing the potential for a very lightweight hand. This work does not represent a completed product able to be used either as a prosthetic device or as gripper for a robot, but a step in that direction.

Some of the first mechanical hands were part of body-powered artificial limbs with a mechanical hook or claw type end effector. Powered mechanical hands have seen some significant advances since these hands were considered state of the art. These advances have occurred primarily in prosthetics applications. An ideal solution for replacing a human hand is still far from being realized. Possibly one of the reasons this is true is that the two primary design criteria for prosthetic hands are often conflicting ones. Because the hand is part of the body, it is unique to each person. Likewise, the ideal replacement for the human hand would also be unique to each user. On the other hand, any prototype device has to be a solution that is well accepted by enough users to warrant developing it into a marketable product [5]. Although there are many advanced hands under development, none of them incorporates all of the advancements that research has produced. Many of them implement advanced control schemes and sensors to achieve a significant level of automation, but many of the most advanced hands still do not have five powered fingers [6–11]. Carrozza et al. [12] proposed the SPRING hand that features underactuated mechanisms. Pons et al. [13] presented the MANUS-HAND that also uses the underactuated principle. None of them has as many fully actuated DOFs as the human hand, an attribute which of course, an ideal replacement for the human hand would have. These deficiencies are probably due to compromises made to save weight and to reduce the complexity of controlling a greater number of DOFs.

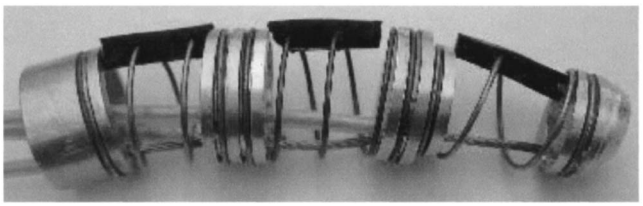

Fig. 3 Entire finger assembly

Many commercially available hands, such as the Otto Bock SensorHand™, only have three digits, usually the thumb, index, and middle fingers, and have two or three DOFs, which are coupled together, and actuated by one motor. Hands such as these are only capable of being used for a cylindrical grasp or chuck grasp. These grasps result from the same motion of the hand and are only differentiable depending on the size of the object and it position within the grasp. Such hands have only limited functional use [14].

Design and Prototyping of the Hand Mechanism

The key feature of this hand mechanism is its joint mechanism used for the finger joints. Unlike all other mechanical hands, which employ solid links with revolute joints or another conventional mechanism, this one makes use of a flexible element made up primarily of a compression spring. This spring comprises most of the structure for each finger segment, but it is also this flexible element that provides motion for the flexion and extension DOF of the finger. Each finger is made up of a series of three springs connected in series that are held in place by short aluminum finger segment links. Each segment, in the current design, has one DOF and is actuated by a single cable. Although, each joint currently has only one DOF to replicate the extension and flexion of the human finger, more cables could be added at appropriate orientations around certain finger segments to add additional DOFs; the DOFs would replicate the adbuction and adduction motion of the human finger. The DOF of the fingers of the human hand are described in Fig. 1.

Figure 2 depicts a computer aided design model of a typical joint segment that would be used to make up a finger. This segment includes a spring and the cable and conduit used to actuate the segment. Two aluminum finger segment links at either end are

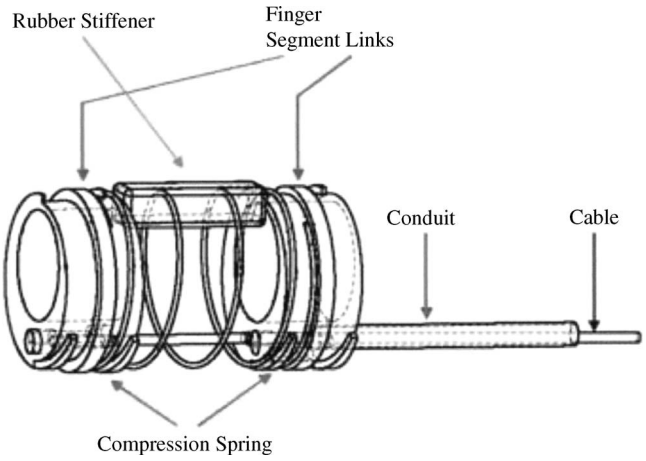

Fig. 2 Finger segment with cable and conduit

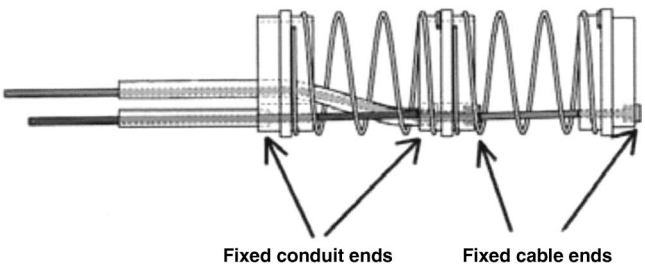

Fig. 4 Cable routing for two segments

Table 1 Spring properties

Spring properties					
Joint	Outside spring diameter o.d. (mm)	Wire diameter d(mm)	Length L(mm)	Number of active coils n	Spring constant k(N/mm)
1-1	18.0	0.965	22	2	6.9
1-2	22.0	0.927	19	3	3.9
1-3	22.0	1.016	21	2.1	9.1
2-1	13.6	0.610	21	4	0.3
2-2	17.7	0.737	20	5	0.6
2-3	21.0	0.914	32	5	2.5
3-1	12.7	0.762	19	5	1.2
3-2	13.6	0.622	20	4.5	0.4
3-3	17.7	0.724	33	9.5	0.1
4-1	12.7	0.699	21	5	0.7
4-2	13.6	0.610	23	4.5	0.6
4-3	17.7	0.699	25	5.5	0.1
5-1	10.6	0.622	19	6	0.4
5-2	12.7	0.737	21	5.25	0.8
5-3	15.8	0.838	20	3.3	2.7

used to connect the spring to the springs in the preceding and following segments and to retain the ends of the cable and conduit. The finger segment links have a thread-like structure at each end that in effect screws into the first coil of the compression spring, holding the spring securely.

The joint segment also includes a rectangular rubber block, or stiffener, that runs the length of the compression spring opposite of the cable. The purpose of the stiffener is twofold, to resist axial compression of the spring and to resist hyperextension of fingers, which ensures a desirable deformed shape of the fingers when tension is applied to the cables. These characteristics are due to the fact that the rubber material that is between each coil of the spring has a much higher resistance to compression than the compression spring itself. Given that Young's modulus for rubber ranges from approximately 7×10^{-4} and 4×10^{-3} GPa and the cross-sectional area of the average size stiffener, it can be found that the stiffness coefficient of the average stiffener in terms of a Hooke's law relationship is between 22 and 130(N/m). The stiffness coefficient of the average spring used is approximately 1.3(N/m). Therefore the finger segments are roughly one to two orders of magnitude stiffer in terms of axial compression and hyperextension of the fingers as compared to a normal flexion motion. These stiffness values refer to the stiffener and spring considered independently in axial compression only. A more detailed explanation of the importance of spring stiffness in presented below.

Fifteen finger segments similar to those shown in Fig. 1 were developed to comprise an entire five-fingered hand with three segments in each of the four fingers and the thumb to make a total of 15 DOFs. The mechanical thumb is capable of bending in extension and flexion at the carpometacarpal, the metacarpophangeal (MCP), and the interphangeal joints. Each mechanical finger is capable of bending in flexion and extension at the MCP, the proximal interphalangeal (PIP), and the distal interphalangeal (DIP) joints.

Figure 3 shows one entire finger unit with three finger segments and three cable and conduit sets to actuate all the segments. The tip of the thumb is located towards the right of the Fig. 3. On the left of Fig. 3 is the thumb base, which slips into the aluminum hand body fixture. Each finger can be added to and removed from the rest of the hand as one unit. The finger segment link closest to the hand for each finger is cylindrical for the majority of its length and fits with a slip fit into cylindrical holes in the hand body. The hand body is also constructed of aluminum and designed to resemble the shape of a hand. The fingers are arranged in a configuration that resembles human anthropometry thus the hand mechanism is suitable for grasping. The other four fingers are constructed in a similar fashion.

The cables and conduits run from the finger segment that they actuate, through the empty space in the center of the preceding elements, continue through the hollow finger bases, and exit though the bottom of the hand body fixture. This arrangement allows for a single segment to be actuated without affecting the other two segments located in that finger. Figure 4 shows how a set of cables and conduits would be routed through a series of finger segments. There is a large hole in each finger segment link that multiple cable and conduits sets can run through for the following finger segments. Figure 5 shows the complete hand with three DOFs for each of the five fingers, giving it 15 DOFs.

Without the inclusion of a rubber stiffener, the stiffness of the compression spring itself represents an important tradeoff in the design of a finger segment. The maximum normal force that can be generated between a finger and a grasped object is proportional to the stiffness of the springs in that finger. As the hand closes to grasp an object and a finger first comes into contact with the object, normal force is developed between the finger and the surface of the object. Given that the finger exerts a force on the grasped object, there is a corresponding equal and opposite force the object exerts on the finger. This force causes the flexing elements to tend to compress on the backside of the finger, opposite of the cable, causing the flexing element to assume a shape of pure axial compression, which is unsuitable for grasping an object. Increasing the stiffness of the springs will increase the maximum amount of normal force that the finger is able to produce and

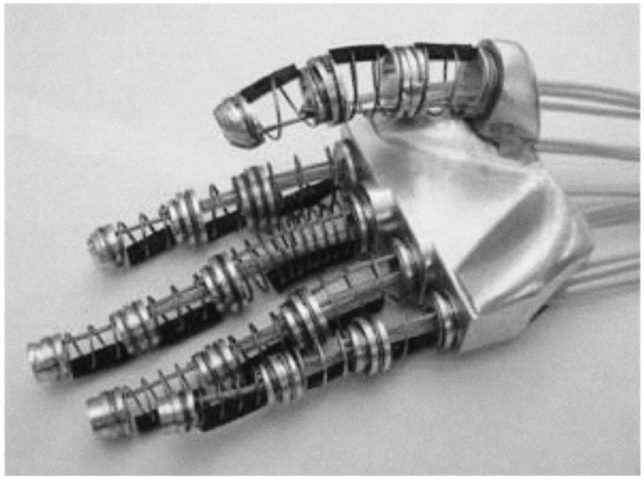

Fig. 5 Entire hand assembly

Table 2 Joint range of motion

Finger	Joint	Minimum joint angle (degrees)	Maximum joint angle (degrees)	Range of motion (degrees)	Rotation (degrees)
Thumb	1-1, interphangeal	22	49	27	200
	1-2, metacarpophalangeal	12	44	32	
	1-3, carpometacarpal	18	49	31	
	total range of motion			90	
Index	2-1, distal interphalangeal	12	83	71	170
	2-2, proximal interphalangeal	12	62	50	
	2-3, metacarpophalangeal	9	66	57	
	total range of motion			178	
Middle	3-1, distal interphalangeal	4	76	72	170
	3-2, proximal interphalangeal	12	72	60	
	3-3, metacarpophalangeal	10	84	74	
	total range of motion			206	
Ring	4-1, distal interphalangeal	13	75	62	200
	4-2, proximal interphalangeal	19	87	68	
	4-3, metacarpophalangeal	0	56	56	
	total range of motion			186	
Little	5-1, distal interphalangeal	17	76	59	130
	5-2, proximal interphalangeal	17	77	60	
	5-3, metacarpophalangeal	15	63	48	
	total range of motion			167	

therefore the maximum grasping force of the entire hand. Greater tension for actuating the hand would be required and therefore necessitate the use of large and more powerful motors for actuation.

The inclusion of a rubber stiffener on the backside of each element is the key to making this finger segment perform in a useful manner for developing a practical gripping device. Using a rubber stiffener to in effect increase the stiffness of the compression spring in only one direction is an innovative solution that simultaneously has the advantages a stiffer spring that can create greater grasping force and a softer spring that is easier to actuate.

Dimensions and the mechanical properties of the springs used are given in Table 1. These are properties of the coil springs themselves and not of bending segments including the rubber stiffeners. Springs were selected on a number of characteristics: fit to the cosmetic glove, length (i.e., middle of spring lengthwise located at appropriate joint location), and stiffness.

Experiments were performed to measure the range of motion of the fingers and fingertip trajectory and orientation. Each finger was measured individually by placing the base of a finger in a clamp and marking the position and orientation of the fingertip as the motors were stepped in small increments. The results are displayed in Table 2 and Fig. 6. Joint angles are defined as the angle of deflection from one end of the spring to the other. They are determined by the orientation of one finger segment link with respect to the previous one. The maximum joint angle refers to the joint angle at full flexion. The minimum joint angle is not usually zero because the at rest position of the fingers is slightly bent instead of straight out from the hand.

These experiments point out that range of motion of the fingers is one area where there is room for improvement in the design of the hand. It is suggested that the total range of motion for the fingers of the human hand is 215 degrees for the thumb and between 270 and 300 degrees for the index, middle, ring, and little fingers [15]. Because of this deficiency, the hand sometime has trouble grasping small objects in certain grasp types, for instance grabbing a pencil in a cylindrical grasp.

Aesthetics

The need to have a realistic, esthetically pleasing device is especially true in the field of prosthetics. For many prosthesis users, the esthetics of a device is just as important as the functionality. The ideal replacement for the human hand is one that perfectly mimics not only the function of the human hand but also the appearance including size, shape, weight, texture, color, and movement. The user of a prosthetic device has to be very comfortable using it and the ideal comfort level naturally includes appearance among other things [5]. To help achieve this ideal, this hand was intentionally designed for use with a cosmetic glove covering it. The glove resembles a human hand and forearm, and this dictated the dimensions of the majority of the components used in the construction of the hand. The diameters of the finger segment links and of the springs were chosen so that they would closely match the inner dimensions of the cosmetic glove. The lengths of springs were carefully chosen so that middle of the spring lengthwise, and therefore the middle of the curve of the deflected finger segment, would coincide with the location of the knuckles of the cosmetic glove. The glove is made of silicone, available in several skin colors, and produced by Ossur. Changes in shape could still be made to the hand's structure to achieve a closer resemblance to the shape of a human hand, especially in the case of the hand body. To achieve the ideal shape for an entire hand assembly, would necessitate a close focus on human hand anthropometry when designing all the components.

Results for the developmental stage of this more realistic mechanical hand have been satisfactory. Figures 7 and 8 compare, respectively, the palm side and the back of the hand of the mechanical hand with a human hand. Each photo shows the human hand on the right, the artificial hand on the left. Although there is some difference in color between the human and cosmetic glove, which is available in many skin tones, the shape of artificial hand does mimic the human hand well, especially considering that improvements could be made with a more anthropometrically driven design.

Static Load-Deformation Analysis of Finger Segments

The linear load-deformation relationship for a small element of the helical spring will first be established without taking the stiffener into account. There are two coordinate systems, the global system denoted by *abc* and the local system denoted by *xyz*. The *a* axis is along the center line of the undeformed element. The *x* axis is along the center line of the wire, The *y* axis is perpendicular to the *a* axis as shown in Fig. 8. The external load is **F**

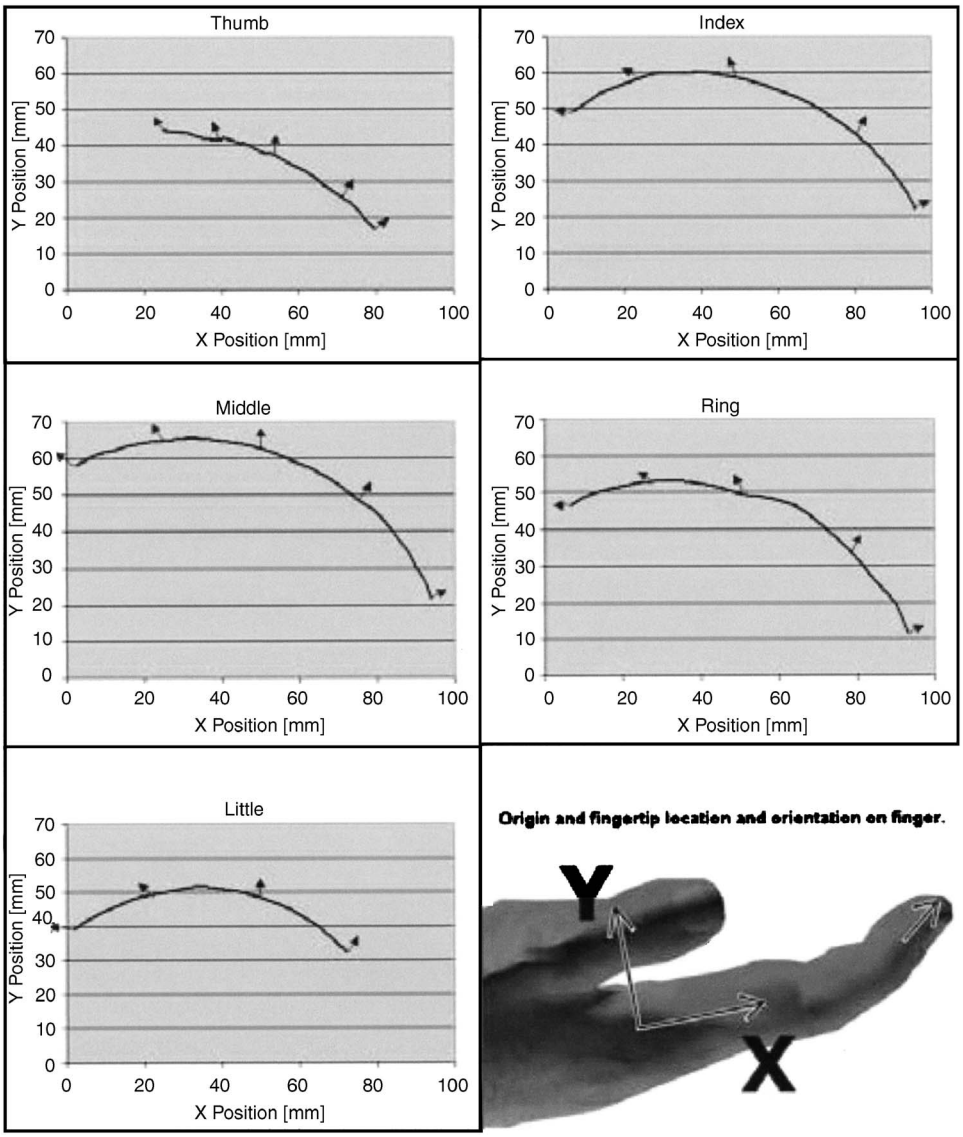

Fig. 6 Fingertip trajectory, arrows specify fingertip orientation along the trajectory (in flexion/extension)

$=[F_a\ F_b\ F_c]^T$ and $\mathbf{M}=[M_a\ M_b\ M_c]^T$ at the bottom center point of the top knuckle. The pitch angle is defined by $\eta=\arctan(L/n\pi D)$ where n is the number of active coils, d is the wire diameter, D is the mean spring diameters, L is the length of the loaded spring.

For one element in Fig. 9, the rotational angle ϕ with respect to the a axis changes from ϕ_1 to ϕ_2. The internal forces and moments at the local coordinate system xyz are obtained using the following transformations:

(a) Translating the action of the force along the global a axis
(b) Rotating it to the direction of the local y axis
(c) Translating it along the local y axis
(d) Rotating it the pitch angle about the local y axis

Therefore the internal forces and moments can now be expressed as the multiplication of the associated transformation matrices as follows:

$$\mathbf{Q}_{xyz}=\mathbf{R}_\eta\mathbf{U}_y\mathbf{R}_\phi\mathbf{U}_a\mathbf{Q}_{abc} \tag{1}$$

where $\mathbf{Q}_{xyz}=[F_x\ F_y\ F_z\ M_x\ M_y\ M_z]^T$, $\mathbf{Q}_{abc}=[F_a\ F_b\ F_c\ M_a\ M_b\ M_c]^T$, and where each matrix is defined in Lindkvist [16]. The elastic energy of the curved beam between angles ϕ_1 and ϕ_2 is defined by Lindkvist [16]

$$U=\int_{\phi_1}^{\phi_2}\left[\frac{\left(F_x+\frac{2M_z}{1+(\tan\eta)^2}\right)^2}{2EA}+\frac{F_y^2}{2kGA}+\frac{M_z^2}{2EJ}+\frac{M_x^2}{2GK}+\frac{F_x^2}{2kGA}+\frac{M_y^2}{2EI}\right]\frac{D}{2\cos\eta}d\phi \tag{2}$$

where E and G are the material elastic normal and tangential modula, respectively,

$$J=\frac{\pi D^4}{8}\left(1-\frac{1}{2}\left(\frac{d}{D}\right)^2-\sqrt{1-\left(\frac{d}{D}\right)^2}\right)$$

and

$$K=\left(1+3\left(\frac{d}{D(1+(\tan\eta)^2)}\right)^2\Big/16\left(1-\left(\frac{d}{D(1+(\tan\eta)^2)}\right)^2\right)\right)\pi d^4/32$$

$$F_x=F_c\cdot\cos\eta\cdot\cos\phi+F_a\cdot\sin\eta+F_b\cdot\cos\eta\cdot\sin\phi \tag{3a}$$

Fig. 7 Artificial and human hand (palm)

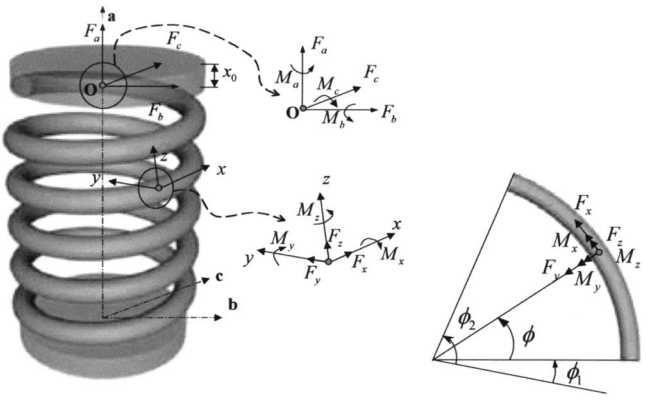

Fig. 9 The spring element and the coordinate systems

$$F_y = -F_b \cdot \cos\phi + F_c \cdot \sin\phi \tag{3b}$$

$$F_z = F_a \cdot \cos\eta - F_c \cdot \cos\phi \cdot \sin\eta - F_b \cdot \sin\eta \cdot \sin\phi \tag{3c}$$

$$M_x = \frac{D}{2}F_a \cdot \cos\eta + M_c \cdot \cos\eta \cdot \cos\phi + M_a \cdot \sin\eta + M_b \cdot \cos\eta \cdot \sin\phi + F_b\left(-\frac{D}{2}(\phi_2 - \phi) \cdot \cos\phi \cdot \sin\eta - \frac{D}{2}\sin\eta \cdot \sin\phi\right) + F_c\left(\frac{D}{2}(\phi_2 - \phi) \cdot \sin\phi \cdot \sin\eta - \frac{D}{2}\sin\eta \cdot \cos\phi\right) \tag{3d}$$

$$M_y = -M_b \cdot \cos\phi + M_c \cdot \sin\phi - \frac{D}{2}F_c(\phi_2 - \phi) \cdot \cos\phi \cdot \tan\eta - \frac{D}{2}F_b(\phi_2 - \phi) \cdot \sin\phi \cdot \tan\eta \tag{3e}$$

$$M_z = M_a \cos\eta - \frac{D}{2}F_a \cdot \sin\eta - M_c \cos\phi \cdot \sin\eta - M_b \sin\eta \cdot \sin\phi + F_b\left(-\frac{D}{2}\cos\eta \cdot \sin\phi + \frac{D}{s}(\phi_2 - \phi)\cos\phi \cdot \sin\eta \cdot \tan\eta\right) + F_c\left(-\frac{D}{2}\cos\eta \cdot \cos\phi - \frac{D}{s}(\phi_2 - \phi)\sin\phi \cdot \sin\eta \cdot \tan\eta\right) \tag{3f}$$

Using the Castigliano theorem, the deformation at the end of the element is

$$\delta d_a^e = \frac{\partial U}{\partial F_a}, \quad \delta d_b^e = \frac{\partial U}{\partial F_b}, \quad \delta d_c^e = \frac{\partial U}{\partial F_c}, \quad \delta\varphi_a^e = \frac{\partial U}{\partial M_a}, \quad \delta\varphi_b^e = \frac{\partial U}{\partial M_b}, \quad \delta\varphi_c^e = \frac{\partial U}{\partial M_c}$$

and if we write in matrix form $\mathbf{q}_{abc}^e = H\mathbf{Q}_{abc}^e$, where $H_{6\times6}$ is the element stiffness matrix [16].

The deflection obtained above characterizes the displacement of the fixed end with respect to the free end resolved in the $x_1y_1z_1$ system. Therefore, it is now necessary to transform it to the coordinate system xyz in Fig. 10(*a*). Indeed, the system $x_1y_1z_1$ is a local coordinate system at the free end of the spring; the system

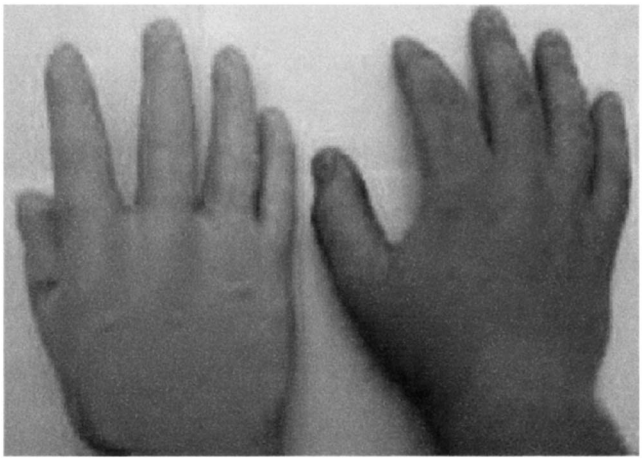

Fig. 8 Back of hand

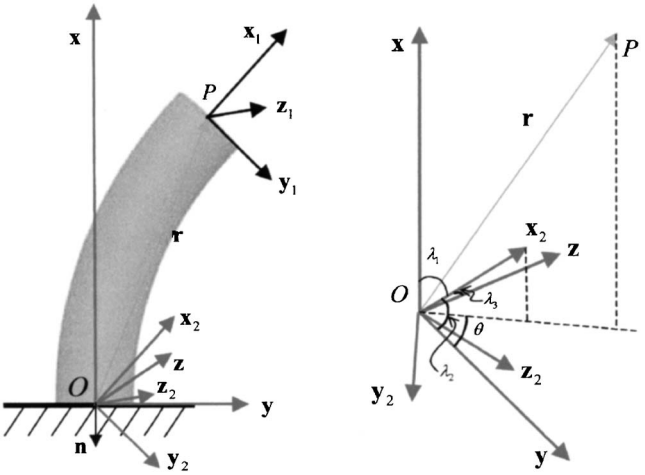

Fig. 10 Coordinate systems (*a*). The relationship of three systems (*b*). *xyz* and $x_2y_2z_2$

$x_2y_2z_2$ is another local coordinate system, which locates at the fixed end, coincides with the origin O of the global coordinate system xyz and has the same orientation of the system $x_1y_1z_1$. The vector $r=[x \quad y \quad z]^T$ is defined in xyz system. Angles α, β, and γ from the element stiffness model are the deflection angles (Euler's angles) at the fixed end in $x_1y_1z_1$ system.

From $x_1y_1z_1$ to $x_2y_2z_2$

$$[x_2 \quad y_2 \quad z_2]^T = -[x_1 \quad y_1 \quad z_1]^T \tag{4}$$

The relationship between the two coordinate system $x_2y_2z_2$ and xyz can be defined by

$$r_{x_2y_2z_2} = Rr_{xyz} \tag{5}$$

where

$$R = \begin{bmatrix} \cos\beta\cos\gamma & -\cos\beta\sin\gamma & \sin\beta \\ \cos\alpha\sin\gamma+\sin\alpha\sin\beta\cos\gamma & \cos\alpha\cos\gamma-\sin\alpha\sin\beta\sin\gamma & -\sin\alpha\cos\beta \\ \sin\alpha\sin\gamma-\cos\alpha\sin\beta\cos\gamma & \sin\alpha\cos\gamma+\cos\alpha\sin\beta\sin\gamma & \cos\alpha\cos\beta \end{bmatrix} \tag{6}$$

Assume the unit vector $x_2=[\cos\lambda_1 \quad \cos\lambda_2 \quad \cos\lambda_3]^T$ and the relationship is shown in Fig. 10(*b*). Therefore, we have the following equations from Fig. 10(*b*)

$$(\cos\lambda_1)^2 + (\cos\lambda_2)^2 + (\cos\lambda_3)^2 = 1 \tag{7a}$$

$$\cos\lambda_3 = \tan\theta\cos\lambda_2 \tag{7b}$$

$$\tan\theta = \frac{z}{y} \tag{7c}$$

$$\lambda_1 = \alpha \tag{7d}$$

The position vector of the free end can be represented in xyz by

$$\begin{Bmatrix} x \\ y \\ z \end{Bmatrix} = \begin{Bmatrix} -x_1\cos\beta\cos\gamma - x_3\sin\beta + x_2\cos\beta\sin\gamma \\ x_3\cos\beta\sin\alpha - x_1(\cos\gamma\sin\alpha\sin\beta + \cos\alpha\sin\gamma) - x_2(\cos\alpha\cos\gamma - \sin\alpha\sin\beta\sin\gamma) \\ -x_3\cos\beta\cos\alpha - x_1(-\cos\alpha\cos\gamma\sin\beta + \sin\alpha\sin\gamma) - x_2(\sin\alpha\cos\gamma + \cos\alpha\sin\beta\sin\gamma) \end{Bmatrix} \tag{8}$$

The final deflection of the free end with respect to the fixed end is defined by

$$\Delta x = L - x \tag{9a}$$

where Δx is the deflection in x direction

$$\Delta y = y \tag{9b}$$

where Δy is the deflection in x direction

$$\Delta z = z \tag{9c}$$

where Δz is the deflection in z direction The three rotation angles are derived as

$$\lambda_1 = \alpha \tag{9d}$$

$$\lambda_2 = \text{Arccos}\left(\sqrt{\frac{1-(\cos\alpha)^2}{1+(z/y)^2}}\right) \tag{9e}$$

$$\lambda_3 = \text{Arccos}\left(\frac{z}{y}\cos\lambda_2\right) \tag{9f}$$

Equations (9*a*)–(9*f*) characterize the resulting motion after applying a force through the cable-conduit to move the upper compression link.

We implement the deformation equations where mechanical properties of the spring element are shown in Table 3.

To run the element stiffness model one can obtain the numerical results and compare them with experiment results in Tables 4–6 as follows, where the unit for the force is Newton (N), the unit for the moment is Newton by meter (N m), and each table shows that

Table 3 The mechanical properties

Wire diameter	d=0.0023 m
Mean spring diameter	D=0.034 m
Number of active coils	n=6
Length of the spring	L=0.036 m
Pitch of the spring	h=0.09549 m
Modulus of Elasticity	E=210 GPa
Stiffness of the compression	$K=Gd^4/8nD^3$
Modulus of rigidity	G=80 GPa

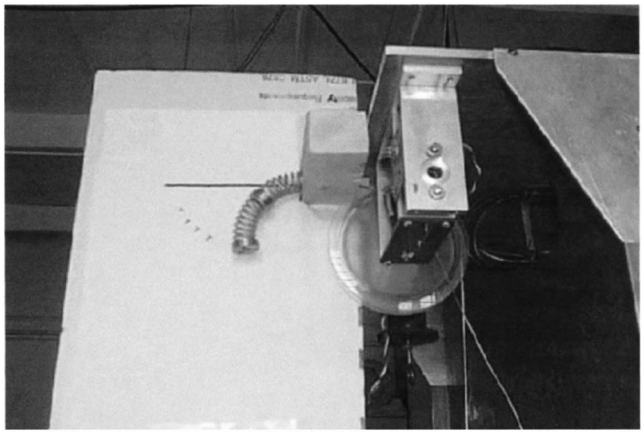

Fig. 11 Experiment setup for a finger of the hand mechanism

it has different external load in the cable-conduit. The results through numerical and experiment methods are close.

A mechanism is set up to test the flexing/load relationship for each mechanical spring (Fig. 11). It includes several parts: a pulley, weight block, a frame fixing the base of finger springs. The loads are supplied by different weights through wires in every knuckle. In our experiment we used three different weights: 1, 5, and 10. The results are shown in Tables 4–6.

The method of loading the compression spring used in this design induces a lateral deflection with a relative translation and rotation of the upper compression link. Recall that the lower compression link is considered fixed because the motions of the different segments of the finger are independent (Fig. 12). This particular aspect of the mechanical spring is what has enabled us to develop a finger-like action, yet maintain the compliant aspect of the hand. Note that both the analytical characterization and the experimental results have been carried out without the rubber stiffener. However, the case with the rubber stiffener is easily derived from the general case without the rubber stiffener.

In Fig. 12, force is transmitted through cable 1. Force 1 is the tension placed on the cable. To exert force 1 on the cable it is necessary to exert an equal and opposite force, force 2, on the conduit. These forces are transmitted through the cable and conduit to each end of segment 1. This results in a pair of compressive forces acting on segment 1 and independent motion of that segment.

Actuation System

Power Transmission. For the current state of development of the hand mechanism, a bench-top actuation system serves well for experimentation and further development. The current hand mechanism reduces the 15 DOFs of the hand to five independent DOFs by coupling together the three DOFs in each finger. Coupling the joints together in this manner allows for a less complex actuation and control system that will allow for development of the mechanical characteristics of the hand itself, such as grasp strength and range of motion. At the same time it will allow for research to be conducted on the concept of coupling the joints in the hand. This is important for two reasons. Fewer motors will allow for a smaller, lighter weight actuation system, which will be a crucial step in refining the hand to a level where it can be used as a prosthetic device. The joints of the human fingers are not coupled together in an exact one-to-one relationship, but there is certainly some coupling that exists. An actuation system that also couples the joints together will lead to a better understanding of this idea.

The actuation system includes the cables that actuate each finger segment and the conduit that houses and routes the cables. The conduit also transmits an equal and opposite force that acts on the segment link on the opposite end of the compression spring as the link upon which the tension from the cable acts. The equal and opposite force restricts the tension in a cable to actuating only the

Table 4 ***Fx*=−6, *Fy*=0, *Fz*=0, *Mx*=0, *My*=−0.051, *Mz*=0.051**

$x1$(mm)	$y1$(mm)	$z1$(mm)	α(degree)	β(degree)	γ(degree)
−30.7	2.0	2.3	0.6	6.7	-6.9
x(mm)	y(mm)	z(mm)	λ_1(degree)	λ_2(degree)	λ_3(degree)
30.8	1.6	1.3	0.5	89.5	89.6
Δx(mm)	Δy(mm)	Δz(mm)	$\Delta\lambda_1$(degree)	$\Delta\lambda_2$(degree)	$\Delta\lambda_3$(degree)
5.1	1.6	1.3	0.6	89.5	89.6
			Experiment results		
5.1	1.5	1.2	⋯	⋯	⋯

Table 5 ***Fx*=−9, *Fy*=0, *Fz*=0, *Mx*=0, *My*=−0.102, *Mz*=0.051**

$x1$(mm)	$y1$(mm)	$z1$(mm)	α(degree)	β(degree)	γ(degree)
−27.9	1.9	4.2	1.0	12.9	−6.8
x(mm)	y(*mm*)	z(*mm*)	λ_1(degree)	λ_2(degree)	λ_3(degree)
28.2	1.3	2.2	1.0	89.4	89.1
Δx(mm)	Δy(mm)	Δz(mm)	$\Delta\lambda_1$(degree)	$\Delta\lambda_2$(degree)	$\Delta\lambda_3$(degree)
7.7	1.3	2.2	1.0	89.4	89.1
			Experiment results		
7.7	1.3	2.1	⋯	⋯	⋯

Table 6 ***Fx*=−12, *Fy*=0, *Fz*=0, *Mx*=0, *My*=−0.051, *Mz*=0.153**

$x1$(mm)	$y1$(mm)	$z1$(mm)	α(degree)	β(degree)	γ(degree)
−25.2	5.4	2.2	1.3	5.8	−19.3
x(mm)	y(*mm*)	z(mm)	λ_1(degree)	λ_2(degree)	λ_2(degree)
25.7	3.2	0.4	1.3	88.6	89.8
dx(mm)	dy(mm)	dz(mm)	$\Delta\lambda_1$(degree)	$\Delta\lambda_2$(degree)	$\Delta\lambda_3$(degree)
10.2	3.2	0.4	1.3	88.6	89.8
			Experiment Results		
10.1	3.2	0.4	⋯	⋯	⋯

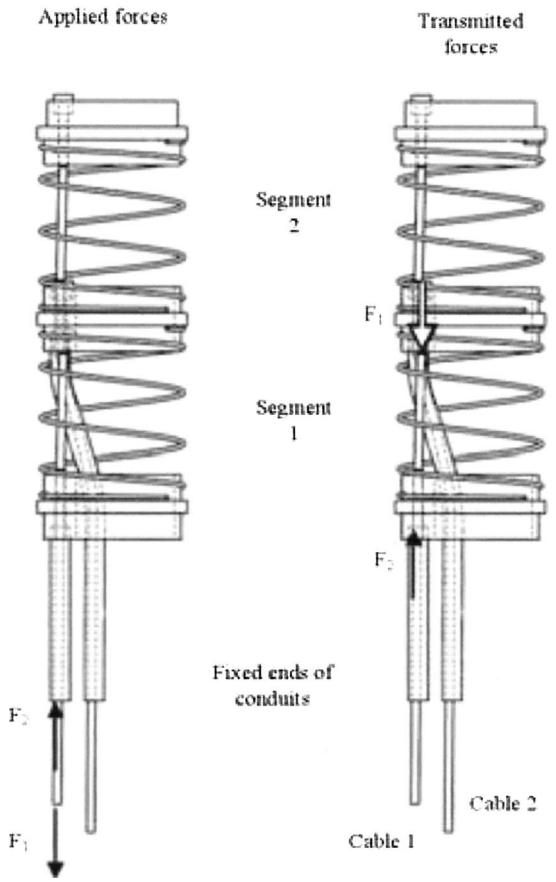

Fig. 12 Force transmission through cable 1

intended finger segment. The actuation system also contains five stepper motors which each turn three pulleys; each pulley turn actuates one cable each. The rest of the actuation system consists of assorted hardware to connect three pulleys to each motor and to connect one cable to each pulley, and a fixture to hold all of the motors and pulleys. Finally, 15 cable adjusters individually adjust the pretension in each cable in order for all three cables in one finger to begin to displace all the finger segments simultaneously.

To reduce cost and complexity for this stage of development, the joints are coupled to reduce the DOFs of the actuation system for the hand. The coupling is achieved by actuating all three DOFs for each finger with one stepper motor that rotates three pulleys. The circumferences of the pulleys were varied with respect to each other according to the maximum displacement of the cable necessary to draw the corresponding finger segment to its maximum defection. This way, the three finger segments in a given finger would be at the same percentage of full deflection at all times. All three segments would begin to move simultaneously. They would also reach their maximum displacement simultaneously at one orientation of the motor. Coupling the joints in this manner provides a motion that is similar to natural human flexion and extension of the fingers because human DIP and PIP joints move in a coupled manner as well.

The joint mechanisms are actuated by a series of cables and conduits that allow the motors that actuate the joints to potentially be located off the hand, also increasing the potential for a very light weight hand. There are several options for the locations of the actuators. In any case the actuation system would need to be made more efficient so that smaller, lighter motors could be used and the entire actuation system could be contained in a smaller, more ergonomic package. The first option would be in the palm of the hand. For this option the motors would have to be extremely small, since there would still likely be at least five motors. This would also increase the weight of the hand mechanism and locate the center of mass of the device further away from the users shoulder. The second option would take advantage of fact that the forces are transmitted through flexible cable conduit pairs and locate the motors completely off of the limb. The motors could be clustered in an ergonomic package that is worn somewhere else on the body, possibly in a pack worn around the waist. The cables could then run from the pack, under the clothes, to the hand. The advantage would be that much of the weight could be located completely off of the limb, minimizing the burden on the user. The disadvantage would be the addition of another component to the system that the user would have to wear. If the amount of residual limb allowed for it, the third option would be a compromise between the first two options. This would be to locate the motors in the forearm or wrist space. This would locate the weight further up the user's limb reducing the perceived weight of the device and eliminate the need for an additional pack to be worn.

Performance Requirements. The first requirement to consider is the amount of force it takes to displace the fingers to full flexion and how much torque is required of the motors to exert this much force on the cables. This is the minimum force required to produce the posture with the tightest grip. Additional force will need to be generated in order to produce significant normal force on the surface of a grasped object. It is also just as important to consider the pulley radii that will be used with the motors, as this will give a direct relationship between the force and torque necessary to pull the cables. Table 7 lists the force necessary to displace each joint to full displacement and the total force necessary to displace each finger. Also listed is the required torque for the pulley sizes used.

Another consideration to take into account is the maximum and minimum change in orientation that the motor will be expected to make in one movement. Since the average draw required is less the one inch of cable (listed in Table 7) and the draw for any individual finger segment is less than the circumference of the corresponding pulley, no motor needs to rotate the output shaft of the gearbox an entire 360 deg. Therefore the movements that require the highest angular velocities are very short in duration, less than 1s if the hand is to mimic the rate at which a human can go from full extension to full flexion. Because of this, a motor that can accelerate and decelerate quickly (quickly enough to reach an average angular velocity of greater than one revolution per second) is required for movements as quick as a human, whereas, when humans grasp and manipulate and object many times very precise movements of the fingers are required. Therefore a motor that can be precisely positioned is also necessary. Since no other dedicated device, such as an electrically triggered brake, is used to maintain cable tension in static loading situations, an additional requirement of the actuation system is that the motors provide a means to stabilize and hold the position of the hand when it is just maintaining a posture or grasping an object.

Motors and Control Setup. For the experimentation and development stage a system that is easily reconfigurable and expandable has obvious advantages. The overall control and actuation system consists of stepper motors, stepper motor drives, a power supply, a motion controller PCI card located in a host desktop personal computer (PC) and the interconnect module. Five NEMA size-17, bipolar, hybrid, 1.8 deg, direct current (dc) stepper motors equipped with 3.6:1 gear reduction via an offset spur gear provide mechanical power for the hand. Five RMS Technologies, R208 microstepping drives power the motors (Table 8). The drives receive direction and velocity commands from the controller and then energize the windings of motor accordingly. The electrical power is provided by two variable voltages (0 to 15 V), 40 A DC power supplies connected in series, providing variable voltage over the input range of the drives (12–24 V). The motion controller is DMC-1850 five-axis motion controller that resides in the PCI Bus of a standard desktop PC. It has its own micropro-

Table 7 Force (applied to cable) and torque required to fully deflect each joint

Torque required to reach full flexion of fingers						
Joint	Cable displacement to maximum deflection mm (in.)	Max load per finger segment N (lbs)	Max load per finger N (lbs)	Pulley radius mm (in.)	Torque per joint N m (oz in.)	Total torque per finger N m (oz in.)
1-1	20.1(0.79)	14.7(3.3)		4.3(0.170)	0.063(8.9)	
1-2	20.1(0.79)	9.3(2.1)	40.9(9.2)	4.3(0.170)	0.040(5.7)	0.17(24.6)
1-3	19.1(0.75)	17.3(3.9)		4.1(0.162)	0.071 (10)	
2-1	22.1(0.87)	10.7(2.4)		5.0(0.198)	0.054(7.6)	
2-2	21.1(0.83)	6.7(1.5)	36.0(8.1)	4.8(0.189)	0.032(4.5)	0.16(23.0)
2-3	18.0(0.71)	18.7(4.2)		4.1(0.162)	0.077(10.9)	
3-1	18.0(0.71)	14.7(3.3)		4.1(0.162)	0.060(8.5)	
3-2	20.1(0.79)	10.7(2.4)	81.4(18.3)	4.6(0.180)	0.048(6.8)	0.49(69.8)
3-3	30.0(1.18)	56.0(12.6)		6.9(0.270)	0.385(54.5)	
4-1	17.0(0.67)	12.5(2.8)		4.4(0.175)	0.054(7.7)	
4-2	16.0(0.63)	48.5(10.9)	81.0(18.2)	4.1(0.162)	0.199(28.2)	0.41(57.7)
4-3	30.0(1.18)	20.0(4.5)		7.7(0.303)	0.154(21.8)	
5-1	17.0(0.67)	13.8(3.1)		4.4(0.175)	0.060(8.5)	
5-2	17.0(0.67)	21.8(4.9)	60.1(13.5)	4.4(0.175)	0.097(13.8)	0.26(36.7)
5-3	16.0(0.63)	24.9(5.6)		4.1(0.162)	0.102(14.4)	

cessor and memory and performs all of the motion commands internally without using the computers resources. The interconnect module is basically an extension of the motion controller and provides terminals to handle all of the input/output (I/O) for the motion controller. This includes committed I/O for each axis along with several digital and analog inputs and outputs, which allows for a great deal of expandability ideal for this stage of development.

This system provides excellent performance characteristics, in terms of angular resolution, holding and running torque, acceleration, suitable for actuating the hand mechanism. The angular resolution of the motors allows for very precise control of the cable displacement and, therefore, hand posture. The current actuation and control system provides an excellent means of actuating the hand for the purpose of developing and refining the hand mechanism itself. Further refinement of the actuation system must be made before it is suitable to be worn as part of a prosthetic device.

These torque and velocity figures refer to torque and velocity after gear reduction and not torque and velocity of the motor itself. Holding torque, or the torque the motor provides to keep the hand static, is critical to maintaining a grasp. The holding torque produced when the maximum current is supplied to the windings while the motor is stationary would be approximately equal to the maximum running torque, but the friction associated with the gear reduction increases this amount. The amount of torque produced provides tension on the cables that is quite sufficient (over twice the amount required for full deflection of the fingers) for posturing the hand and providing gripping force. Any amount of current up to the maximum rated current of the motor can be passed through the windings of a stepper motor to produce holding torque. The drives used have an automatic current cutback feature that can be enabled, which automatically reduces the current to 23% of the maximum current setting during holding conditions. This reduces the rate of energy consumption and still provides excellent holding torque. When no power is supplied to the motors, there is a small amount of holding torque still present due to the magnetic interaction of the magnetized rotor and the stators of the motor. This torque is multiplied by the gear reduction, however it is insufficient to provide enough gripping force in most situations.

Motion Control. The user can send explicit keyboard commands to the controller for execution such as specific relative position moves with a defined acceleration, deceleration, and velocity. This of course, is a very basic way of controlling the hand and is only useful for developmental purposes. This method does not allow for the possibility of executing a coordinated series of motions. Fortunately, there is a software development kit provided with the controller that allows interaction with an executable written in any one of a number of programming languages.

One of the most difficult aspects of developing a hand mechanism that could potentially be used as the major component of a prosthetic system with a large number of DOFs is a user interface. Many currently available prosthetics use myoelectric signals from the residual muscles to control grasping. However, for a user to consciously control more than one or two DOFs individually, is too mentally complex and would make the device too cumbersome to use. Control of a large number of DOFs is impossible unless some sort a hierarchical control scheme can be developed to simplify the commands the user must provide and coordinate many DOFs. A motion control system that used this sort of control scheme would receive just a few high level commands from the user and then send many coordinated low level commands to the motor that govern the motion of the hand. This sort of motion control scheme would be most useful when it was given additional

Table 8 Actuation system specifications

Motor (rotating)	Drive (stationary)	Maximum angular resolution (degrees)	Maximum linear resolution of cable (mm)
Lin Engineering NEMA size 17, 1.8 degree stepper with 3.6:1 gear reduction	RMS Technologies R208	0.5	0.036
1.06 (N m) max running torque, 0.81 (N m) at 2 rev/s	Microstepping, current limiting	0.0625	0.0045

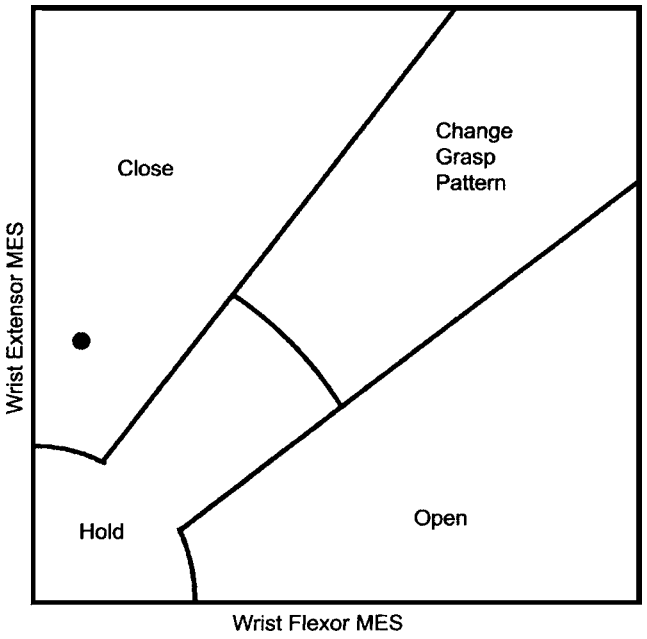

Fig. 13 State activation chart (see Ref. [17])

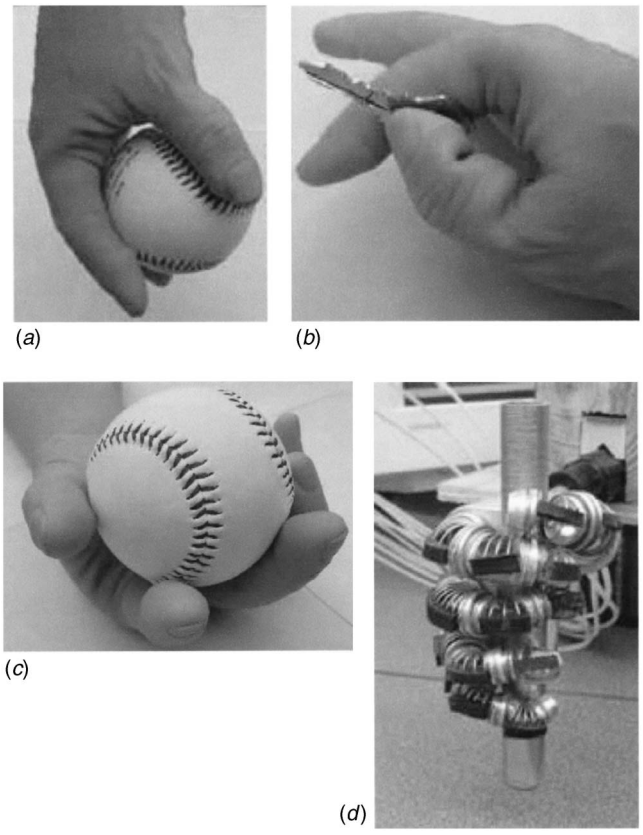

Fig. 14 (*a*) Grasping a ball, (*b*) grasping a key, (*c*) grasping a ball, (*d*) grasping a cylinder

information other than input form the user, such as feedback from sensors that could be embedded in the hand. For instance, pressure sensors could be embedded in the inside surface of the fingers and the surface of the palm and be used to signal to motion control system when contact with an object has been made [6,9]. In fact, a hierarchical control scheme is probably necessary for any prosthesis with more than just one or two degrees of freedom.

One hierarchical control scheme was explored to evaluate the capabilities of the hand and demonstrate its use in a real-world application. Knutson et al. [17] developed a control scheme simulating state activation of a neuroprosthesis using two myoelectric signals, from the wrist extensor and flexor muscles. Sensors were implanted in patients' wrist flexor and extensor muscles, and then both myoelectric signals were monitored. The flexor myoelectric signal was then used to represent an x coordinate; the extensor myoelectric signal was used to represent a y- coordinate, which together corresponded to a location on a state activation chart (Fig. 13).

The signal space is divided into four regions, "Hold," "Open," "Close," and "Change Grasp Pattern." When the Hold command is active, which corresponds to both sets of muscles being at rest, the hand mechanism stays in its current posture. When the extensor muscles are excited, the Close command is activated, which causes the hand to tighten its grasp. Likewise, when the flexor muscles are excited, the Open command is activated widening the grasp. When both sets of muscles are excited, the Change Grasp Pattern command is activated; it can be used to toggle between different grasping postures, such as cylindrical, spherical, pinch, and key grasps. These grasps could be ordered in a series. Each time the control point moves from another region into the Change Grasp Pattern region the next grasp patter in the series could be activated, allowing the user to cycle through the series in order to select the desired grasp.

To incorporate this control scheme to operate the hand, software was developed to use a joystick to simulate the myoelectric signals. The joystick, which contains two linear potentiometers that are each manipulated by one DOF of the joystick, is connected to the interconnect module. The voltage across the two potentiometers is monitored. One DOF simulates the extensor myoelectric signal, while the other simulates the flexor myoelectric signal in the same manner as the above-mentioned neuroprosthesis. Proportional control has been developed by bringing into correspondence the distance traveled into either the Open or Close regions with how far the hand opens or closes. Joint limits are also incorporated.

Posture and Grasping. While the 15 DOFs of the current hand make the hand more complex than currently available hand devices, it is still far less than the human hand's 25 DOFs [18]. More DOFs, such as abduction and adduction of the fingers, could be obtained by adding more cables to some of the finger segments. These cables would then be simultaneously actuated to control flexion—extension as well as abduction—adduction [19]. This addition would greatly expand the grasping and posturing capabilities of the hand, although the inherent compliance of the flexible finger segments enables grasping of objects to work very well (Figs. 14(*a*)–14(*d*)).

The cylinder shown in Fig. 14(*d*) is a steel bar that weights approximately 350 and is 19 mm in diameter. The bar has two different surface finishes, a smooth one and a rough one. When only the smooth surface is gripped, the bar will slip if it is held in the vertical position. The bar stops slipping as soon as the rougher surface slides in between the index finger and thumb. However, this test was conducted with out the use of the cosmetic glove, which has a much higher coefficient of friction than the aluminum surface of the hand. This suggests an approximate minimum grasping force of over 5 N.

One potential problem in situations similar to the one shown in Fig. 14(*d*), is that the weight of the grasped object can exert enough force on the fingers to cause enough deflection in the fingers perpendicular to the flexion/extension plane that the grasp will fail or the fingers deflect in an unnatural position. This is not the case in the test shown here, however, further tests would have to be conducted to determine the maximum weight that the hand is capable of holding in such a position.

Conclusions and Discussions

A 15 DOF prototype hand mechanism has been developed which has potential as a prosthetic devise or human hand-like gripper for a robotic system. A computer-controlled bench-top actuation system has also been developed, which will be used for further development. A simulation of a potential control strategy has been implemented which simplifies control of the hand. This device has advantages over existing hand mechanisms, such as a potential for less overall weight and for a higher number of DOFs, which will enable a more natural reproduction of hand movements and grasping postures.

This greater realism should greatly increase use and usefulness of the device, as the hand is also more aesthetically pleasing than many currently available models. The static load-deformation analysis of finger segments has been completed and the experiment setup built. The simulation and experimental results and the simulation have been shown to be very close.

There are still lots of issues to solve towards final commercial hand prosthesis. During the design and prototyping stage, maximum grasping forces, grasp stability, and cosmetic glove restrictions are important aspects to investigate. The friction of the cables with the conduits and the contact forces with objects should be considered during deformation analysis. Dynamics analysis is necessary to study. Finally, pattern identification plays a key role in the implementation of hand prosthesis grasping.

References

[1] Atkins, D., Heard, D., and Donovan, W., 1996, "Epidemiologic Overview of Individuals with Upper Limb Loss and Their Reported Research Priorities," Journal of Prosthetics and Orthotics, Vol. **8**, No. 1, 2–11.

[2] Schulz, C., Pylatiuk, G., and Bretthauer, A., 2001, "A New Ultralight Anthropomorphic Hand," *IEEE Conference on Robotics and Automation*, pp. 2437–2441.

[3] Massa, B., Roccella, S., Carrozza, M. C., and Dario, P., 2002, "Design and Development of an Underactuated Prosthetic Hand," *Proceeding of the 2002 IEEE International Conference on Robotics & Automation*, Washington, DC.

[4] Hirose, S., Kado, T., and Umetani, Y., 1983, "Tensor Actuated Elastic Manipulator," *Proceedings of the 6th IFToMM World Congress*, New Delhi, Vol. **2**, pp. 978–981.

[5] Kyberd, P., Chappell, P., and Gow, D., 2003, "Advances in the Control of Prosthetic Arms," Technology & Disability; **15**(2), pp. 57–61.

[6] Butterfass, J., Hirzinger, G., Knoch, S. and Liu, H., 1998, "DLR's Multisensory Articulated Hand. Part I: Hard- and Software Architecture," *Proceedings of the 1998 IEEE International Conference on Robotics & Automation*, Leuven, Belgium.

[7] Kyberd, P. and Chappell, P., (1994), "The Southampton Hand: An Intelligent Myoelectric Prosthesis," J. Rehabil. R. D, Vol. **31**, Issue 4, 326–334.

[8] Kyberd P., Light, C., Chappell, P., Nightingale, J., Whatley, D., and Evans, M., 2001, "The Design of Anthropomorphic Prosthetic Hands: A Study of the Southampton Hand," Robotica, **19**, pp. 593–600.

[9] Tura, A., Lamberti, C., Davalli, A., and Sacchetti, R., 1998, "Experimental Development of a Sensory Control System for an Upper Limb Myoelectric Prosthesis with Cosmetic Covering," J. Rehabil. R. D, **35**(1), pp. 14–26.

[10] Carrozza, M. C., Dario, P., Vecchi, F., Roccella, S., Zecca, M., and Sebastiani, F., 2003, "The CyberHand: On the Design of a Cybernetic Prosthetic Hand Intended To Be Interfaced To the Peripheral Nervous System," *Proceedings, 2003 IEEE/RSJ International Conference on Intelligent Robots and Systems.*

[11] Zecca, M., Cappiello, G., Sebastiani, F., Roccella, S., Vecchi, F., Carrozza, M. C., and Dario, P., 2003 "Experimental Analysis of the Proprioceptive and Exteroceptive Sensors of an Underactuated Prosthetic Hand," *Proceeding of the ICORR 2003 (The Eighth International Conference on Rehabilitation Robotics).*

[12] Carrozza, M. C., Suppo, C., Sebastiani, F., Massa, B., Vecchi, F., Lazzarini, R., Cutkosky, M. R., and Dario, P., 2004, "The SPRING Hand: Development of a Self-Adaptive Prosthesis for Restoring Natural Grasping," Auton. Rob., **16**(2), pp. 125–141.

[13] Pons, J. L., Rocon, E., Ceres, R., Reynaerts, D., Saro, B., Levin, S., and Van Moorleghem, W., 2004, "The MANUS-HAND Dextrous Robotics Upper Limb Prosthesis: Mechanical and Manipulation Aspects," Auton. Rob., **16**(2), pp. 143–163.

[14] Yang, J., Abdel-Malek, K., and Potratz, J., 2005, "Design and Prototyping of an Active Hand Prosthetic Device," Ind. Robot, **32**(1), pp. 71–78.

[15] Peña Pitarch, E., Yang, J., and Abdel-Malek, K., 2003, "Santos™ Hand: A 25-Degree-of-Freedom Model," *Proceedings of SAE Digital Human Modeling for Design and Engineering*, 14–16 June, 2005, Iowa City, IA.

[16] Lindkvist, L., 1995, *Three-Dimensional Load-Deformation Relationships of Arbitrarily Loaded Coiled Springs*, Chalmers University of Technology, Goteborg, Sweden.

[17] Knutson, J., Hoyen, H., Kilgore, K., and Peckham P., 2004, "Simulated Neuroprosthesis State Activation and Hand-Position Control Using Myoelectric Signals from Wrist Muscles," J. Rehabil. R. D, **41**(3B), pp. 461–472.

[18] Savescu, A., Cheze, L., Wang, X., Beurier, G., and Verriest, J., 2004, "A 25 Degrees of Freedom Hand Geometrical Model for Better Hand Attitude Simulation," *Proceedings of the Digital Human Modeling for Design and Engineering Symposium*, Rochester, MI.

[19] Yang, J., Peña Pitarch, E., Abdel-Malek, K., Patrick, A., and Lindkvist, L., 2004, "A Multi-Finger Hand Prosthesis," Mech. Mach. Theory, **39**(6), pp. 555–581.